

OBLITERATION DYNAMICS IN CEREBRAL ARTERIOVENOUS MALFORMATIONS AFTER CYBERKNIFE RADIOSURGERY: QUANTIFICATION WITH SEQUENTIAL NIDUS VOLUMETRY AND 3-TESLA 3-DIMENSIONAL TIME-OF-FLIGHT MAGNETIC RESONANCE ANGIOGRAPHY

Berndt Wowra, M.D.

European CyberKnife Center,
Munich-Grosshadern,
Munich, Germany

Alexander Muacevic, M.D.

European CyberKnife Center,
Munich-Grosshadern,
Munich, Germany

Jörg-Christian Tonn, M.D.

Department of Neurosurgery,
Ludwigs-Maximilian
University of Munich,
Munich, Germany

Stefan O. Schoenberg, M.D.

Department of Clinical Radiology
and Nuclear Medicine,
Mannheim University Hospital,
Mannheim, Germany

Maximilian Reiser, M.D.

Institute of Clinical Radiology,
Ludwigs-Maximilian
University of Munich,
Munich, Germany

Karin A. Herrmann, M.D.

Institute of Clinical Radiology,
Ludwigs-Maximilian
University of Munich,
Munich, Germany

Reprint requests:

Berndt Wowra, M.D.,
European CyberKnife Center,
Max-Lebsche-Platz 31,
81377 Munich, Germany.
Email: Berndt.Wowra@cyber-knife.net

Received, April 9, 2008.

Accepted, October 13, 2008.

Copyright © 2009 by the
Congress of Neurological Surgeons

OBJECTIVE: To investigate the time-dependent obliteration of cerebral arteriovenous malformations (cAVM) after CyberKnife radiosurgery (CKRS) (Accuray, Inc., Sunnyvale, CA) by means of sequential 3-T, 3-dimensional (3D), time-of-flight (TOF) magnetic resonance angiography (MRA), and volumetry of the arteriovenous malformation (AVM) nidus.

METHODS: In this prospective study, 3D TOF MRA was performed on 20 patients with cAVMs treated by single-fraction CKRS. Three-dimensional TOF MRA was performed on a 3-T, 32-channel magnetic resonance scanner (Magnetom TIM Trio; Siemens Medical Solutions, Erlangen, Germany) with isotropic voxel size at a spatial resolution of $0.6 \times 0.6 \times 0.6 \text{ mm}^3$. The time-dependent relative decay of the transnidus blood flow evidenced by 3D TOF MRA was referred to as "obliteration dynamics." Volumetry of the nidus size was performed with OsiriX imaging software (OsiriX Foundation, Geneva, Switzerland). All patients had 3 to 4 follow-up examinations at 3- to 6-month intervals over a minimum follow-up period of 9 months. Subtotal obliteration was determined if the residual nidus volume was 5% or less of the initial nidus volume. Stata/IC software (Version 10.0; Stata Corp., College Station, TX) was used for statistical analysis and to identify potential factors of AVM obliteration.

RESULTS: Regarding their clinical status, case history, and pretreatments, the participants of this study represent difficult-to-treat cAVM patients. The median nidus volume was 1.8 mL (range, 0.4–12.5 mL); the median minimum dose prescribed to the nidus was 22 Gy (range, 16–24 Gy) delivered to the 67% isodose line (range, 55–80%). CKRS was well tolerated, with complications in 2 patients. No further hemorrhages occurred after RS, except 1 small and clinically inapparent incident. The median follow-up period after RS was 25.0 months (range, 11.7–36.8 months). After RS, a statistically significant obliteration was observed in all patients. However, the obliteration dynamics of the cAVMs showed a pronounced variability, with 2 types of post-therapeutic behavior identified. cAVMs of Group A showed a faster reduction of transnidus blood flow than cAVMs in Group B. The median time to subtotal obliteration was 23.8 months for all patients, 11.6 months for patients in Group A, and 27.8 months for patients in Group B ($P = 0.05$). Logistic regression analysis revealed dose homogeneity and the circumscribed isodose to be the only variables ($P < 0.01$) associated with the obliteration dynamics in this study. The cumulative complete angiographic obliteration rate was 67% (95% confidence interval, 32–95%) 2 years after RS.

CONCLUSION: The use of sequential 3D TOF MRA at 3 T and nidus volumetry enables a noninvasive quantitative assessment of the dynamic obliteration process induced by CKRS in cAVMs. This method may be helpful to identify factors related to AVM obliteration after RS when larger patient cohorts become available.

KEY WORDS: 3-dimensional time-of-flight magnetic resonance angiography, 3-Tesla magnetic resonance imaging, Cerebral arteriovenous malformation, CyberKnife, Dynamic obliteration, Frameless robotic image-guided radiosurgery

ABBREVIATIONS: **AVM**, arteriovenous malformation; **cAVM**, cerebral arteriovenous malformation; **CI**, confidence interval; **CK**, CyberKnife; **CKRS**, CyberKnife radiosurgery; **DSA**, digital subtraction angiography; **GKRS**, gamma knife radiosurgery; **MRA**, magnetic resonance angiography; **MRI**, magnetic resonance imaging; **RS**, radiosurgery; **3D**, 3-dimensional; **TOF**, time of flight

Stereotactic radiosurgery (RS) is acknowledged to be a valuable treatment principle for cerebral arteriovenous malformations (cAVM) (35, 36). The relatively long latency to achieve complete obliteration of the malformation is a feature of RS of cAVMs that is generally regarded as a specific disadvantage (25, 32). Determinants of the obliteration latency are generally unknown.

The unequivocal diagnostic work-up of cAVMs is based on digital subtraction angiography (DSA). However, the use of invasive DSA after cAVMs have been treated by RS is limited by low patient acceptance. With magnetic resonance angiography (MRA), noninvasive evaluation of cAVMs becomes feasible (10). The applicability of 3-dimensional (3D) time-of-flight (TOF) MRA for treatment planning and follow-up of radiosurgically treated cAVMs has previously been shown (20, 38). Magnetic resonance imaging (MRI) at 3 T represents the pinnacle of current clinical imaging. High 3-T field strengths increase the signal gain and allow for MRI with higher spatial resolution and shorter acquisition time. Recently, the CyberKnife (CK) RS (CKRS) system (Accuray, Inc., Sunnyvale, CA) has been introduced as advanced treatment technology for RS (1). The CK enables frameless robotic image-guided RS. Integration of 3-T MRI scans into the dose-planning process of CKRS and its use for sequential follow-up studies would be very attractive. In fact, this approach could transform RS for cAVMs into a completely noninvasive therapeutic concept.

Given this background, we intended to primarily evaluate the response of cAVMs to CKRS using 3D TOF MRA at 3-T field strength and to quantify the size of the arteriovenous malformation (AVM) nidus with sequential volumetry with this study. Here, we refer to the time-dependent decay of the transnidus blood flow after RS as “obliteration dynamics.”

PATIENTS AND METHODS

The CK robotic RS system consists of a 6-MV compact linear accelerator mounted on a computer-controlled, 6-axis robotic manipulator (1, 23). Integral to the system are orthogonally positioned x-ray cameras for image acquisition during treatment. These images are processed automatically to identify specific cranial structures. The information is then referenced to the treatment planning computed tomographic study, and the exact position of the RS target (e.g., the nidus of the cAVM) is determined in real time. Thus, the system is able to compensate for changes in patient position during treatment. The treatment principle of the CK represents a noncoplanar, nonisocentric dose delivery. The precision of the CK technology is comparable to published localization errors in current frame-based RS systems (7).

In general, a high prescription dose of between 15 and 25 Gy is needed to obliterate cAVMs by RS. CK treatment plans show excellent homogeneity, conformity, and target coverage (8). The homogeneity

index is the ratio of the maximum dose to the prescription dose. Homogeneity of the dose distribution is better at smaller values of the homogeneity index.

A Magnetom TIM Trio (Siemens Medical Solutions, Erlangen, Germany) fully integrated 3-T system with 32 channels and a dedicated 12-channel head coil was used. The standard imaging protocol included T2-weighted fast spin echo sequences, fluid-attenuated inversion recovery, and T1-weighted fast spin echo sequences before and after contrast medium application, as well as a nonenhanced 3D TOF sequence. High-resolution 3D TOF MRA was acquired using a 3D fast low-angle shot sequence (gradient recalled echo) with isotropic voxel size and a spatial resolution of $0.6 \times 0.6 \times 0.6 \text{ mm}^3$ (repetition time, 24 ms; echo time, 4.1 ms; bandwidth, 190 Hz/pixel; flip angle, 15 degrees; matrix size, 240×320 ; transverse orientation). For this study, only the 3D TOF sequence was analyzed. All other MRI sequences that were also applied to the patients were disregarded in this study. For every patient, the MRI scans were fused to contrast-enhanced computed tomographic images to verify correct anatomic and cAVM topography during dose planning and to compensate for any potential image distortions in the MRA.

Volumetry of the nidus was performed with OsiriX image processing software (Version 2.7.5; OsiriX Foundation, Geneva, Switzerland). In patients with previous embolization, glue caused spotted, sharply demarcated areas of flow void in the 3-T, 3D TOF MRA. Areas of glue were excluded from nidus volumetry. All MRA images in this study were free of metallic artifacts.

For volumetry, the area of the high-intensity signal indicating blood flow within the AVM nidus was outlined and summed over the whole stack of images containing the nidus. These measurements were performed using the axial source data of the 3D TOF MRA. For data analysis, the initial volume of the AVM nidus was set to 100% for each patient. Nidus volumes measured during sequential examinations were expressed as a percentage of the initial volume and related to 4 distinct follow-up intervals. They were referred to as T_0 through T_4 , with T_0 indicating the date of the CK treatment. Subtotal obliteration of the cAVMs was assumed if the residual nidus volume was 5% or less of the nidus volume at T_0 . Three to 4 follow-up examinations at 3- to 6-month intervals over a minimum follow-up period of 9 months were acquired. Stata/IC software (Version 10.0; Stata Corp., College Station, TX) was used for statistical analysis. Two-group mean comparison tests (*t* tests) were used to assess potential differences in variables according to AVM Groups A and B (defined below according to the latency and rapidity of AVM obliteration). Logistic regression analysis was used to identify potential factors related to differences in obliteration dynamics between Groups A and B. Kaplan-Meier estimates were used to examine the cumulative probability of subtotal and complete obliteration of radiosurgically treated cAVMs.

After RS, the patients underwent prospective sequential MRI at 3- to 6-month intervals. The standard imaging protocol included morphological imaging and 3D TOF MRA before contrast material application. All patients gave informed consent. No patients with contraindications for MRI or MRI contrast agents were included. Furthermore, patients were censored if they had less than 9 months of follow-up after CKRS and fewer than 3 follow-up examinations. If 3D TOF MRA was indicative of complete obliteration of the AVM, a DSA was proposed to the patient to verify complete AVM obliteration.

RESULTS

Over the course of 1.5 years, starting in July 2005, a consecutive series of 20 patients with cAVMs underwent outpatient

CKRS at the European CyberKnife Center in Munich. All patients were treated with single-fraction RS. For patients with primary RS (n = 12), the selection criterion was the finding of a cAVM in eloquent areas of the brain which rendered the lesion inoperable. Two of these patients were re-treated with the CK after previous gamma knife radiosurgery (GKRS) because of persistent nidus. One of the GKRS patients (cAVM in the left cerebellar peduncle) hemorrhaged 2 months before GKRS, and the other (AVM in the left basal ganglia) hemorrhaged 20 months before GKRS. The interval between GKRS and CKRS was 4.8 and 11.3 years, respectively. The nidus volumes were 0.7 and 4.0 mL for GKRS and 0.6 and 0.8 mL for CKRS, respectively. Marginal doses of 22.5 and 20 Gy were prescribed to the 50% isodose line in GKRS, and 20 Gy to the 65% isodose and 18 Gy to the 70% isodose in the CKRS. Six patients were pretreated by endovascular embolization. Surgery was performed to evacuate hemorrhages in 3 patients. One of these patients was embolized before hematoma evacuation. The median Spetzler and Martin score (34) was 4 (range, 3–6), and the median RS AVM score, according to Pollock and Flickinger (30), was 1.34 (range, 0.46–2.4). Fourteen patients (85%) presented with a permanent neurological deficit, 4 with epilepsy, and 4 with distinctive psychopathological features. There were only 3 patients free of AVM-related symptoms. The clinical data are summarized in Table 1.

A total of 20 patients met the inclusion criteria (Table 1). The median follow-up period after RS was 25.0 months (range, 11.7–36.8 months). The median volume of the untreated AVM nidus detected by 3D TOF MRA was 1.8 mL (range, 0.4–12.5 mL), and the median minimum dose prescribed to the nidus was 22 Gy (range, 16–24 Gy). This dose was delivered to the 67% isodose line (range, 55–80%). The median homogeneity index was 1.46 (range, 1.25–1.81).

Nidus volumetry was performed in these 20 patients according to the schedule provided in Table 2. A total of 76 sequential volume quantification measurements were performed (3 or 4 per patient). Obliteration dynamics could be verified in all patients (Figs. 1 and 2). However, the decrease of the transnidus blood flow showed considerable variability from patient to patient. Volumetric subtotal or complete obliteration of the cAVM ($\leq 5\%$ residual nidus) was detected in 16 patients 25 months after CKRS (Fig. 3). In 4 patients, a partial obliteration that did not reach 95% was verified.

Despite the pronounced variability in this small patient sample, 2 subgroups of AVMs could be identified with respect to the obliteration dynamics. Group A (6 patients) had a rapid regression of the nidus, and Group B (14 patients) showed a delayed response (Table 3; Fig. 3). The median homogeneity index was 1.43 (range, 1.25–1.53) in Group A and 1.53 (range, 1.43–1.82) in Group B ($P < 0.01$). Logistic regression analysis revealed dose homogeneity and the circumscribed isodose to be the only significant variables associated with the obliteration dynamics in treated AVM nidi ($P < 0.01$). The other factors tested (age, sex, nidus volume, AVM score, dose level) were not significant in this statistical model. The median time to subtotal obliteration was 23.8 months for all patients, 11.6 months for

TABLE 1. Characteristics of patients and treatment parameters^a

Characteristics	No.
Patients	
Total (no.)	20
Women/men	12/8
Age, median, y (range)	33.4 (13–50)
Focal neurological deficit before CKRS, no. (%)	17 (85%)
AVM side, left/right	11/9
Spetzler-Martin score, median (range)	4 (3–6)
Radiosurgery grading, median (range)	1.35 (0.46–2.4)
Hemorrhage before treatment (no.)	9
Microsurgery before to CKRS (no.)	3
Endovascular embolization (no.)	6
GKRS before CKRS (no.)	2
CKRS	
Nidus volume, mL (median, range)	1.8 (0.4–12.5)
Minimum dose to nidus, Gy (median, range)	22.0 (15.9–24.0)
Maximum dose to nidus, Gy (median, range)	30.3 (24.3–40)
Circumscribed isodose, % (median, range)	68 (55–80)
Homogeneity index (median, range)	1.46 (1.25–1.81)

^a AVM, arteriovenous malformation; CKRS, CyberKnife radiosurgery; GKRS, gamma knife radiosurgery.

TABLE 2. Schedule and histogram of nidus volumetry^a

Time interval after CKRS	Time (mo) after CKRS (mean \pm standard deviation)	No. of observations ^b	No. of patients ^c
T ₀ ^d	0	20	20
T ₁	3.6 \pm 1.0	6	6
T ₂	6.9 \pm 1.3	16	16
T ₃	13.3 \pm 1.9	20	20
T ₄	22.2 \pm 3.6	14	18

^a CKRS, CyberKnife radiosurgery.

^b One observation = 1 nidus volume determination on 3-dimensional time-of-flight magnetic resonance angiography.

^c Number of patients available for nidus volumetry with reference to treatment date. There were a total of 76 measurements.

^d Treatment date.

patients in Group A, and 27.8 months for patients in Group B ($P = 0.05$) (Fig. 3). At this point in time, 7 patients have undergone DSA to investigate occlusion of the AVM. Complete angiographic obliteration was confirmed in 5 patients and subtotal angiographic obliteration in 2. In this regard, the

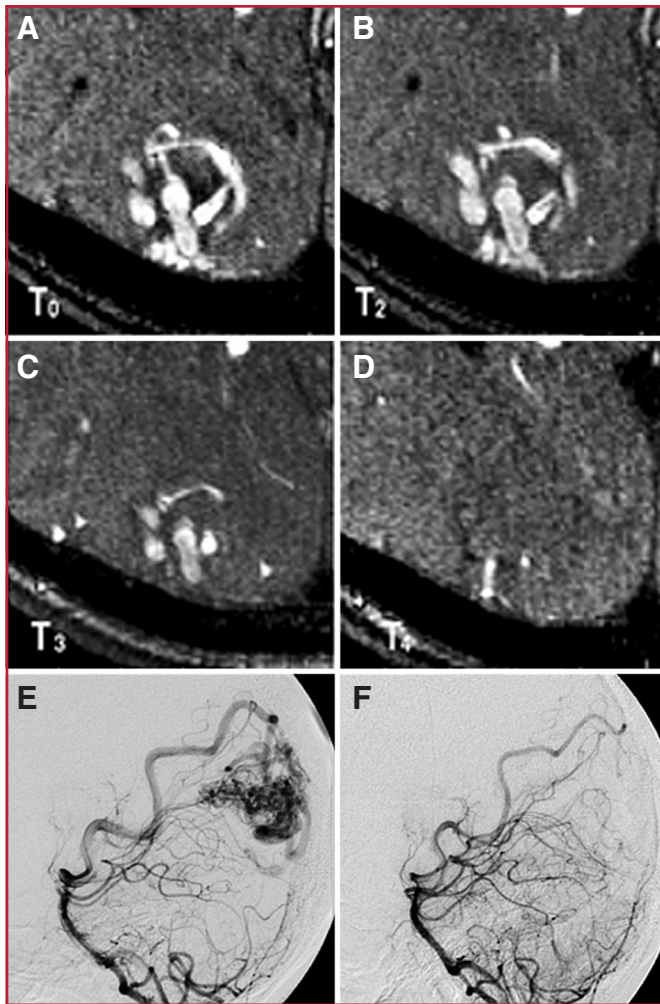


FIGURE 1. Illustrative case of a cerebral arteriovenous malformation (cAVM) in the right occipital lobe treated by CyberKnife radiosurgery (CKRS) (Patient 253). **A–D**, 3-T, 3-dimensional (3D) time-of-flight (TOF) magnetic resonance angiography (MRA). Images are taken at interval T_0 (nidus volume = 7.7 mL [100%]); T_2 (7 months after CKRS; nidus volume = 5.2 mL [67%]); T_3 (12 months after CKRS; nidus volume = 2.5 mL [33%]); T_4 (19 months after CKRS; nidus volume = 0.2 mL [3%]); interval T_1 is not available in this case. **E** and **F**, lateral projections of digital subtraction angiography (DSA) before (left DSA, interval T_0) and 19 months (right DSA, interval T_4) after CKRS. There is almost complete obliteration, corresponding well to the 3-T, 3D TOF MRA. The example is a slowly obliterating cAVM.

cumulative complete obliteration rate was 67% (95% confidence interval [CI], 32–95%) 2 years after CKRS. The corresponding obliteration probabilities obtained for these patients by application of the prediction models developed by Karlsson et al. (19) and Flickinger et al. (15) were 71% (95% CI, 60–74%) and 77% (95% CI, 49–84%), respectively.

CKRS was well tolerated in the majority of patients. Complications of RS were observed in 2 young patients with large cAVMs (nidus volume, 5.6 and 12.5 mL, respectively). Both

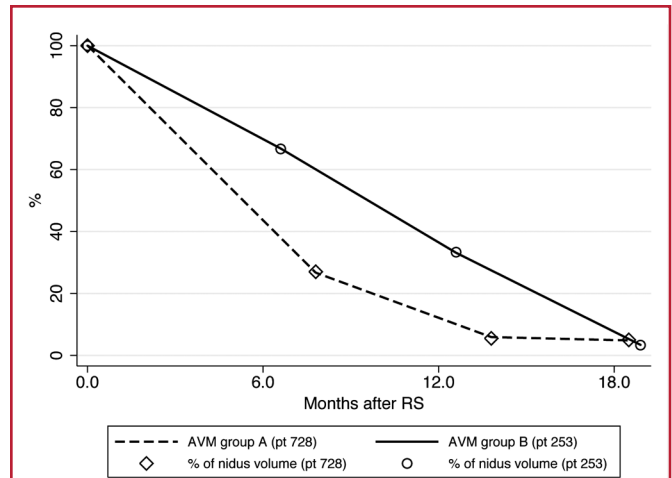


FIGURE 2. Graph showing time-dependent obliteration of cAVMs after CKRS. Two patients with different obliteration dynamics (Patient [pt] 728 of the fast-obliterating Group A; Patient 253 of the slowly obliterating Group B). RS, radiosurgery; AVM, arteriovenous malformation.

individuals were Grade 6 according to Spetzler and Martin, and their RS-based grade was 1.6 and 2.4 (30, 34). The 2 patients had progressive neurological symptoms before RS and there were no other treatment options left for them. One patient experienced a small, clinically silent hemorrhage observed on MRI 3 months after CKRS. This resolved spontaneously. The other patient developed a moderate hemiparesis, probably because of occlusion of a peripheral parietal artery, 6 months after CKRS. The disability has not affected his work status, and he is being treated with physiotherapy.

DISCUSSION

Patients

cAVMs are inhomogeneous with respect to their symptomatology, angioarchitecture, topography, size, and transnidus blood flow. Microsurgery, endovascular surgery, and RS are established methods to free patients from the risk of cerebral hemorrhage that is, to variable degrees, associated with such lesions. Grading or classification systems have been developed as a means to predict the therapeutic risk in relation to surgery, endovascular therapy, and RS (30, 34, 37). Today, the majority of cAVMs can be treated with 1 of the available options alone, or with combination therapy. Nevertheless, there are cAVMs that are still difficult to treat. In the present study, no low-grade cAVMs (34) were included. Patients were characterized by a high median AVM grade of 4 (range, 3–6), according to the Spetzler and Martin (34) classification, and a high RS-based grading score of 1.35 (range, 0.46–2.4); more than 50% of patients had been treated previously (by surgery, endovascular therapy, and/or GKRS) (30, 34). Nine patients had had hemorrhages before treatment. Furthermore, 2 young patients with

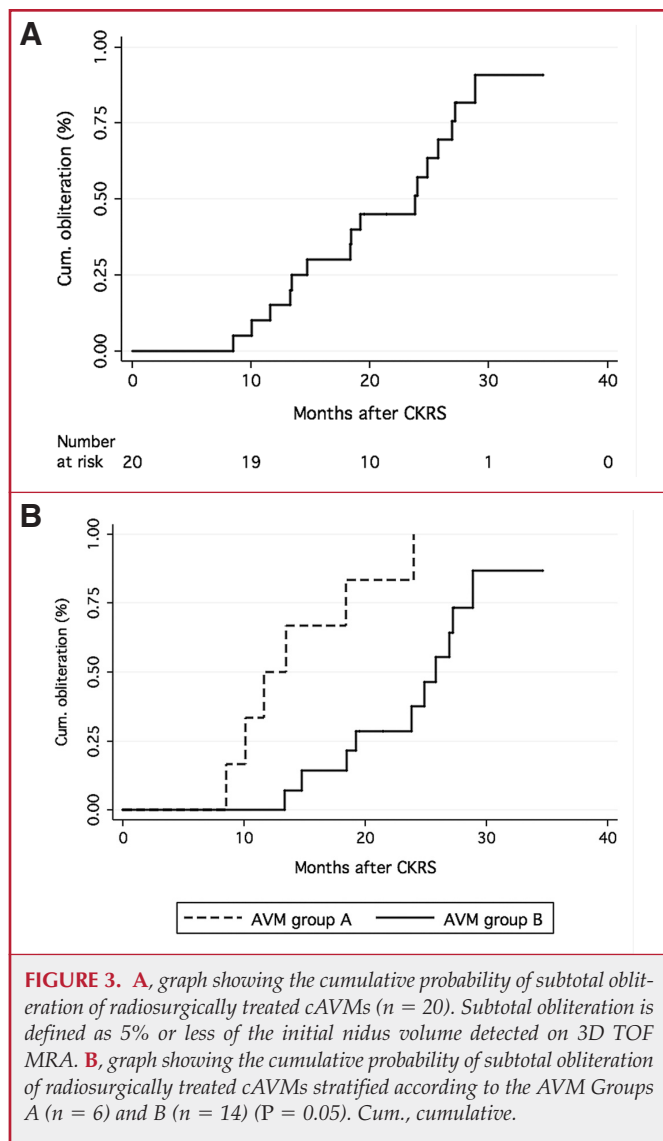


FIGURE 3. A, graph showing the cumulative probability of subtotal obliteration of radiosurgically treated cAVMs ($n = 20$). Subtotal obliteration is defined as 5% or less of the initial nidus volume detected on 3D TOF MRA. **B**, graph showing the cumulative probability of subtotal obliteration of radiosurgically treated cAVMs stratified according to the AVM Groups A ($n = 6$) and B ($n = 14$) ($P = 0.05$). Cum., cumulative.

large cAVMs, progressive symptoms, and no other treatment options were included on the basis of individual informed consent. In this regard, the patients in this study represent a selection of cAVMs that were difficult to treat. Therefore, the observation of a single instance of permanent moderate hemiparesis and 1 asymptomatic hemorrhage as the only side effects may be regarded as acceptable treatment toxicity.

Homogeneity and Strength of the Magnetic Field

Theoretically, medical progress should lead to improved treatment options. In this study, for the first time, with the 3-T Magnetom TIM Trio and the CK, 2 advanced technologies are combined in a prospective study of the treatment of cAVMs. There are several potential pros and cons associated with the 3-T imaging technology. The narrow and long gantry of the 3-T Magnetom TIM Trio provides a very homogeneous

magnetic field. This is of essential importance for treatment planning with the CK, because distortions of the magnetic field could cause inaccurate dose delivery (33). According to our experience, image distortion is a critical issue when using data generated by MRI scanners with short and wide gantries. However, with the 3-T Magnetom TIM Trio system, we did not observe image distortion in this series of AVM patients. In our patients, even the smallest nidus of 0.4 mL was identified in the 3D TOF MRA. The field homogeneity and a 100% detection rate of AVM nidi are true improvements, as compared with the status in 1992, when we were the first to describe the use of 3D TOF MRA for treatment planning and follow-up in RS (11, 20, 33, 38). At that time, corrections of the spatial distortions of the MRI scans were necessary (33). An analog context may account for the observation of others that MRA-based dose planning may miss parts of the AVM nidus and that the nidus contoured on MRA may be displaced with respect to CT imaging or DSA (2, 4). Our experience with 3-T, 3D TOF MRA does not support this statement.

3-T 3D TOF MRA and DSA

It is commonly accepted that DSA remains the “gold standard” for characterization of AVMs (17, 18, 41). It is also desirable to integrate DSA directly into the target definition process during RS dose planning. Previous DSA showing the cAVM was available for all patients in this study. However, the CK software cannot directly process DSA images; therefore, the correlation between DSA and 3D TOF MRA was a matter of principal concern. Bednarz et al. (3) studied the advantages of 1.5-T, 3D TOF MRA, as an adjuvant to DSA, in obtaining 3D information about a cAVM nidus and in optimizing RS treatment plans. The authors concluded that 3D TOF MRA as a complementary imaging modality to DSA increased the accuracy of the AVM RS and allowed for optimal dose planning. As a matter of principle, MRI at high field strengths enables shorter acquisition times and improved spatial resolution. 3-T TOF MRA offers superior characterization of cAVM angioarchitecture, as compared with 1.5-T TOF MRA (18). However, the image quality of MRA at both 3.0 and 1.5 T was still found to be far from equal to DSA (18). Zhang et al. (41) addressed the issue of sensitivity and specificity concerning MRA and DSA for cAVM RS planning and evaluation in a methodical study. They estimated the specificities and sensitivities of MRA and DSA to be (0.95, 0.74) and (0.71, 0.95), respectively. The positive overlap of MRA and DSA accounted for $67.8 \pm 4.9\%$ of the estimated true AVM volume. Compared with plans targeting MRA- and DSA-positive overlap area, plans targeting MRA-positive volume or DSA-positive area improved the cAVM obliteration rate by $4.1 \pm 1.9\%$ and $15.7 \pm 8.3\%$, while also increasing the complication rate by $1.0 \pm 0.8\%$ and $4.4 \pm 2.3\%$, respectively. The authors concluded that aiming at the MRA-positive target (as we did in analogy) is superior to aiming at the MRA and DSA overlap. Nevertheless, they claimed to include DSA in the dose planning process because the target definition is more consistent and robust in combination with DSA, and because of the high sensitivity of DSA (41). Apart

TABLE 3. Characteristics of arteriovenous malformation subgroups^a

Characteristics	Group A ^b	Group B ^c	P value
Patients			
Total (no.)	6	14	NS
Women/men	2/4	10/4	NS
Age, median, y (range)	26.2 (19.3–44.2)	35.5 (13.0–49.8)	NS
AVM side, left/right	4/2	7/7	NS
Spetzler-Martin score, median (range)	4 (3–6)	4 (3–6)	NS
Radiosurgery grading, median (range)	1.23 (0.46–1.56)	1.41 (0.68–2.4)	NS
Hemorrhage before treatment (no.)	4	5	NS
Microsurgery before CKRS (no.)	1	2	NS
Endovascular embolization (no.)	1	5	NS
GKRS before CKRS (no.)	0	2	NS
CKRS			
Nidus volume, cm ³ (mean ± SD)	1.35 (0.4–6.8)	1.8 (0.51–2.5)	NS
Minimum dose to nidus, Gy (mean ± SD)	23.4 (19–24)	20.5 (16–24)	NS
Maximum dose to nidus, Gy (mean ± SD)	30.3 (27–37)	30.4 (24–40)	NS
Circumscribed isodose, % (mean ± SD)	70 (65–80)	65 (55–75)	<0.01
Homogeneity index (median, range)	1.42 (1.25–1.54)	1.54 (1.43–1.81)	<0.01
Obliteration of AVM (nidus)			
Interval T0: nidus volume, %	100	100	
Interval T1: residual nidus, %, (mean ± SD)	27.8 ± 13.1	80.4 ± 20.9	<0.01
Interval T2: residual nidus, %, (mean ± SD)	10.6 ± 14.4	63.1 ± 19.2	<0.001
Interval T3: residual nidus, %, (mean ± SD)	6.6 ± 8.9	26.4 ± 20.6	<0.02
Interval T4: residual nidus, %, (mean ± SD)	1.7 ± 2.8	9.8 ± 13.5	NS

^a NS, not significant; AVM, arteriovenous malformation; CKRS, CyberKnife radiosurgery; GKRS, gamma knife radiosurgery; SD, standard deviation.

^b Rapid nidus obliteration.

^c Slow nidus obliteration.

from the fact that the CK software cannot read DSA images, our experience concerning dose planning with DSA and 3-T, 3D TOF MRA was in agreement with the results of these authors. Furthermore, we found a good correlation between DSA and 3-T, 3D TOF-MRA concerning cAVM obliteration. Thus far, 7 patients have undergone DSA after verification of at least 95% reduction of transnidus blood flow in 3-T, 3D TOF MRA. Complete angiographic obliteration could be demonstrated in 5 and subtotal angiographic obliteration in 2 of these patients. A cumulative, complete obliteration rate of 67% (95% CI, 32–95%) 2 years after CKRS was determined. This is in agreement with the obliteration rates of 50 to 90% published in the literature (6, 14, 19, 21, 24, 26, 28, 29, 31, 40) and with the predicted obliteration rates calculated with the models developed by Karlsson et al. (19) and Flickinger et al. (15).

Obliteration Dynamics

3D TOF MRA is known to provide a very sensitive image of the transnidus blood flow (20). This is the first study to quantify the decay of the transnidus blood flow in a series of

patients with cAVMs treated by CKRS. The time-dependent regression of transnidus blood flow after RS, or obliteration dynamics, is a determinant of the latency period. With 3D TOF MRA, we were able to observe obliteration dynamics in all patients in this study, regardless of the nidus size and whether or not the patient had previous hemorrhage, surgery, endovascular treatment, or no previous therapy. However, a pronounced scattering of the measured values was detected by sequential nidus volumetry after RS. This was not only true of the directly measured volumes, but also applied to the relative (e.g., percentage) numbers, allowing interpatient comparison. In principle, patients could fall into one or the other group because of either treatment-related parameters or biological factors, or some combination. However, probably in part because of the limited sample size, only dose homogeneity and the circumscribed isodose were identified as statistically decisive parameters differentiating the 2 distinct groups of cAVM. AVMs were obliterated faster if the dose distribution was more homogeneous. This finding contributes to the controversy regarding the significance of dose homogeneity in

the radiosurgical literature (5, 16, 22, 39). Some authors claim that inhomogeneity of the dose distribution is not relevant or even positively correlated with AVM obliteration after RS, whereas others take the contrary position.

Limitations of the Study

The present study was based on 3D TOF MRA for practical reasons. However, there are other valuable MRI sequences and techniques available, such as contrast-enhanced, time-resolved MRA and blood bolus tagging techniques to study flow dynamics within the AVM nidus and nidus obliteration after RS (9, 12, 13, 27). In general, such studies hold promise of a better understanding of the effects of RS in cAVMs and to identify biological factors and treatment parameters related to nidus obliteration and the latency period after RS.

The basic concept of this study was to perform entirely non-invasive diagnostic imaging and treatment and to analyze the therapeutic effects of CKRS for cAVM by a simple and practical approach. However, in addition to the small sample size, the authors are aware of further limitations of this study, including incomplete follow-up with DSA and the principal limitations of 3D TOF MRA. More data are required to establish a firm correlation between 3D TOF MRA and DSA to determine the end point of obliteration of the cAVM.

3D TOF MRA is known to depend on flow characteristics, velocity, and flow direction. Flow-related effects may influence the absolute measurements of nidus volumes. Furthermore, 3D TOF MRA may be susceptible to structures with short T1 time and susceptibility artifacts (9). Contrast-enhanced 3D TOF-MRA could compensate for some of these effects. However, venous overlay may hamper the exact volume analysis of the nidus, which is why we preferred imaging before contrast media application. Susceptibility artifacts may be even more pronounced with 3-T imaging, and the degree of impairment and effect on volumetry is not clear. However, using the relative percentage values of sequential volumetry, as we did in this study, these drawbacks of 3D TOF MRA may be minimized, at least for interpatient analysis.

3D TOF MRA does not include dynamic information on the flow characteristics of the nidus. Multiple attempts have been made to quantify the flow dynamics of AVMs with MRI techniques such as blood bolus tagging techniques and contrast-enhanced dynamic studies (9, 12). These techniques are very promising to further understand the hemodynamics of these complex entities. Studies are warranted to further assess these novel techniques and potentially compare the results to nonenhanced 3D TOF MRA.

CONCLUSION

Here, for the first time with the 3-T Magnetom Trio and the CK, 2 advanced noninvasive technologies are combined in a prospective study of difficult-to-treat cAVMs. The time-dependent regression of the transnidus blood flow after RS, referred to as obliteration dynamics, was investigated. With 3D TOF MRA and sequential nidus volumetry, we were able to

quantify obliteration dynamics in all AVM patients with a practical clinical approach. MRA as a noninvasive imaging technique seems to be much more suitable to investigate obliteration dynamics in radiosurgically treated AVM patients than invasive DSA. Two groups of AVM patients were identified, 1 of which showed a faster AVM obliteration rate than the other. The difference between the groups suggests that dose homogeneity is directly related to the speed of AVM obliteration. This pilot study could serve as a template for further noninvasive studies on factors leading to cAVM obliteration after RS.

Disclosure

Berndt Wowra, M.D., is a member of the Clinical Advisory Board of Accuray, Inc., Sunnyvale, CA. Alexander Muacevic, M.D., is a member of the Board of Directors of the CyberKnife Society. The other authors have no personal financial or institutional interest in any of the drugs, materials, or devices described in this article.

REFERENCES

- Adler JR Jr, Chang SD, Murphy MJ, Doty J, Geis P, Hancock SL: The CyberKnife: A frameless robotic system for radiosurgery. *Stereotact Funct Neurosurg* 69:124–128, 1997.
- Aoyama H, Shirato H, Katoh N, Kudo K, Asano T, Kuroda S, Ishikawa T, Miyasaka K: Comparison of imaging modalities for the accurate delineation of arteriovenous malformation, with reference to stereotactic radiosurgery. *Int J Radiat Oncol Biol Phys* 62:1232–1238, 2005.
- Bednarz G, Downes B, Werner-Wasik M, Rosenwasser RH: Combining stereotactic angiography and 3D time-of-flight magnetic resonance angiography in treatment planning for arteriovenous malformation radiosurgery. *Int J Radiat Oncol Biol Phys* 46:1149–1154, 2000.
- Buis DR, Lagerwaard FJ, Dirven CM, Barkhof F, Knol DL, van den Berg R, Slotman BJ, Vandertop WP: Delineation of brain AVMs on MR-angiography for the purpose of stereotactic radiosurgery. *Int J Radiat Oncol Biol Phys* 67:308–316, 2007.
- Chang SD, Adler JR Jr: Current status and optimal use of radiosurgery. *Oncology (Williston Park)* 15:209–221, 2001.
- Chang JH, Chang JW, Park YG, Chung SS: Factors related to complete occlusion of arteriovenous malformations after gamma knife radiosurgery. *J Neurosurg* 93 [Suppl 3]:96–101, 2000.
- Chang SD, Main W, Martin DP, Gibbs IC, Heilbrun MP: An analysis of the accuracy of the CyberKnife: A robotic frameless stereotactic radiosurgical system. *Neurosurgery* 52:140–147, 2003.
- Collins SP, Coppa ND, Zhang Y, Collins BT, McRae DA, Jean WC: CyberKnife radiosurgery in the treatment of complex skull base tumors: Analysis of treatment planning parameters. *Radiat Oncol* 1:46, 2006.
- Duran M, Schoenberg SO, Yuh WT, Knopp MV, van Kaick G, Essig M: Cerebral arteriovenous malformations: Morphologic evaluation by ultrashort 3D gadolinium-enhanced MR angiography. *Eur Radiol* 12:2957–2964, 2002.
- Edelman RR, Wentz KU, Mattle HP, O'Reilly GV, Candia G, Liu C, Zhao B, Kjellberg RN, Davis KR: Intracerebral arteriovenous malformations: Evaluation with selective MR angiography and venography. *Radiology* 173:831–837, 1989.
- Ehrlicke HH, Schad LR, Gademann G, Wowra B, Engenhart R, Lorenz WJ: Use of MR angiography for stereotactic planning. *J Comput Assist Tomogr* 16:35–40, 1992.
- Essig M: Multimodal magnetic resonance diagnostics of arteriovenous malformations [in German]. *Radiologe* 47:884–892, 2007.
- Essig M, Reichenbach JR, Schad L, Debus J, Kaiser WA: High resolution MR-venography of cerebral arteriovenous malformations [in German]. *Radiologe* 41:288–295, 2001.
- Flickinger JC, Kondziolka D, Maitz AH, Lunsford LD: An analysis of the dose-response for arteriovenous malformation radiosurgery and other factors affecting obliteration. *Radiother Oncol* 63:347–354, 2002.

15. Flickinger JC, Pollock BE, Kondziolka D, Lunsford LD: A dose-response analysis of arteriovenous malformation obliteration after radiosurgery. *Int J Radiat Oncol Biol Phys* 36:873–879, 1996.
16. Fuss M, Salter BJ, Caron JL, Vollmer DG, Herman TS: Intensity-modulated radiosurgery for childhood arteriovenous malformations. *Acta Neurochir (Wien)* 147:1141–1150, 2005.
17. Hamm KD, Klisch J, Surber G, Kleinert G, Eger C, Aschenbach R: Special aspects of diagnostic imaging for radiosurgery of arteriovenous malformations. *Neurosurgery* 62 [Suppl 5]:A44–A52, 2008.
18. Heidenreich JO, Schilling AM, Unterharnscheidt F, Stendel R, Hartlieb S, Wacker FK, Schlattmann P, Wolf KJ, Bruhn H: Assessment of 3D-TOF-MRA at 3.0 Tesla in the characterization of the angioarchitecture of cerebral arteriovenous malformations: A preliminary study. *Acta Radiol* 48:678–686, 2007.
19. Karlsson B, Lax I, Söderman M: Can the probability for obliteration after radiosurgery for arteriovenous malformations be accurately predicted? *Int J Radiat Oncol Biol Phys* 43:313–319, 1999.
20. Kauczor HU, Engenhart R, Layer G, Gamroth AH, Wowra B, Schad LR, Semmler W, van Kaick G: 3D TOF MR angiography of cerebral arteriovenous malformations after radiosurgery. *J Comput Assist Tomogr* 17:184–190, 1993.
21. Kemeny AA, Radatz MW, Rowe JG, Walton L, Hampshire A: Gamma knife radiosurgery for cerebral arteriovenous malformations. *Acta Neurochir Suppl* 91:55–63, 2004.
22. Kondziolka D, Lunsford LD, Flickinger JC: The radiobiology of radiosurgery. *Neurosurg Clin N Am* 10:157–166, 1999.
23. Kuo JS, Yu C, Petrovich Z, Apuzzo ML: The CyberKnife stereotactic radiosurgery system: Description, installation, and an initial evaluation of use and functionality. *Neurosurgery* 53:1235–1239, 2003.
24. Liscák R, Vladyka V, Simonová G, Urgosik D, Novotný J Jr, Janousková L, Vymazal J: Arteriovenous malformations after Leksell gamma knife radiosurgery: Rate of obliteration and complications. *Neurosurgery* 60:1005–1016, 2007.
25. Lunsford LD, Kondziolka D, Flickinger JC, Bissonette DJ, Jungreis CA, Maitz AH, Horton JA, Coffey RJ: Stereotactic radiosurgery for arteriovenous malformations of the brain. *J Neurosurg* 75:512–524, 1991.
26. Maruyama K, Shin M, Tago M, Kishimoto J, Morita A, Kawahara N: Radiosurgery to reduce the risk of first hemorrhage from brain arteriovenous malformations. *Neurosurgery* 60:453–459, 2007.
27. Nagaraja S, Lee KJ, Coley SC, Capener D, Walton L, Kemeny AA, Wilkinson ID, Griffiths PD: Stereotactic radiosurgery for brain arteriovenous malformations: Quantitative MR assessment of nidus response at 1 year and angiographic factors predicting early obliteration. *Neuroradiology* 48:821–829, 2006.
28. Nataf F, Merienne L, Schlienger M, Lefkopoulos D, Meder JF, Touboul E, Merland JJ, Devaux B, Turak B, Page P, Roux FX: Cerebral arteriovenous malformations treated by radiosurgery: A series of 705 cases [in French]. *Neurochirurgie* 47:268–282, 2001.
29. Pedroso AG, De Salles AA, Tajik K, Golish R, Smith Z, Frighetto L, Solberg T, Cabatan-Awang C, Selch MT: Novalis shaped beam radiosurgery of arteriovenous malformations. *J Neurosurg* 101 [Suppl 3]:425–434, 2004.
30. Pollock BE, Flickinger JC: A proposed radiosurgery-based grading system for arteriovenous malformations. *J Neurosurg* 96:79–85, 2002.
31. Pollock BE, Gorman DA, Brown PD: Radiosurgery for arteriovenous malformations of the basal ganglia, thalamus, and brainstem. *J Neurosurg* 100:210–214, 2004.
32. Pollock BE, Lunsford LD, Kondziolka D, Maitz A, Flickinger JC: Patient outcomes after stereotactic radiosurgery for “operable” arteriovenous malformations. *Neurosurgery* 35:1–8, 1994.
33. Schad LR, Ehrlicke HH, Wowra B, Layer G, Engenhart R, Kauczor HU, Zabel HJ, Brix G, Lorenz WJ: Correction of spatial distortion in magnetic resonance angiography for radiosurgical treatment planning of cerebral arteriovenous malformations. *Magn Reson Imaging* 10:609–621, 1992.
34. Spetzler RF, Martin NA: A proposed grading system for arteriovenous malformations. *J Neurosurg* 65:476–483, 1986.
35. Steiner L, Leksell L, Greitz T, Forster DM, Backlund EO: Stereotactic radiosurgery for cerebral arteriovenous malformations. Report of a case. *Acta Chir Scand* 138:459–464, 1972.
36. Steiner L, Lindquist C, Cail W, Karlsson B, Steiner M: Microsurgery and radiosurgery in brain arteriovenous malformations. *J Neurosurg* 79:647–652, 1993.
37. Valavanis A, Yaşaril MG: The endovascular treatment of brain arteriovenous malformations. *Adv Tech Stand Neurosurg* 24:131–214, 1998.
38. Wowra B, Engenhart R, Schad LR, Layer G, Kimmig B: Three-dimensional time-of-flight magnetic resonance angiography for treatment planning and follow-up of cerebral arteriovenous malformations after stereotactic irradiation, in Lunsford LD (ed): *Stereotactic Radiosurgery Update*. New York, Elsevier Science Publishing Co., 1992, pp 153–155.
39. Yu C, Jozsef G, Apuzzo ML, Petrovich Z: Dosimetric comparison of CyberKnife with other radiosurgical modalities for an ellipsoidal target. *Neurosurgery* 53:1155–1163, 2003.
40. Zabel-du Bois A, Milker-Zabel S, Huber P, Schlegel W, Debus J: Risk of hemorrhage and obliteration rates of LINAC-based radiosurgery for cerebral arteriovenous malformations treated after prior partial embolization. *Int J Radiat Oncol Biol Phys* 68:999–1003, 2007.
41. Zhang P, Wu L, Liu T, Kutcher GJ, Isaacson S: Incorporate imaging characteristics into an arteriovenous malformation radiosurgery plan evaluation model. *Int J Radiat Oncol Biol Phys* 70:1607–1610, 2008.

Acknowledgment

We thank David Schaal for his help with the English language preparation of this article.

CONTACT THE EDITORIAL OFFICE

To reach the Editorial Office, please use the following information.

NEUROSURGERY

Michael L.J. Apuzzo, Editor
 1420 San Pablo Street, PMB A-106
 Los Angeles, CA 90033
Phone: 323/442-3001
Fax: 323/442-3002
Email: neurosurgery-journal@hsc.usc.edu
Website: www.neurosurgery-online.com